Dalton Transactions

Accepted Manuscript

ROYAL SOCIETY OF CHEMISTRY

www.rsc.org/dalton

Journal Name

COMMUNICATION

Two novel μ_6-O^{2-} bridged Co_{14}/Ni_{14} hydroxamate Clusters packed in distorted face-centered cubic patterns

Received 00th January 2015,
Accepted 00th January 2015

DOI: 10.1039/x0xx00000x

www.rsc.org/

Yanping Zhang, Rui Lv, Jingyao Wang, Linyan Yang, Shengyun Liao, Jinlei Tian, Wen Gu,* Xin Liu*

Two novel clusters $[Co^{II}_{14}(\mu_6\text{-}O^{2-})(sbha)_{12}(sba)_2(DMF)_7(DMA)]\cdot(DMF)_8$ (1) and $[Ni^{II}_{14}(\mu_6\text{-}O^{2-})(sbha)_{12}(sba)_2(DMF)_8]$ (2) (sH_2bha = 4-bromo-benzohydroxamic acid; sHba = 4-bromobenzene carboxylic acid; DMF = N,N-dimethylformamide; DMA = dimethylamine) have been synthesized. The novel body-centred μ_6-O^{2-} bridged Co_{14} and Ni_{14} clusters are packed in distorted face-centered cubic (FCC) patterns with different symmetry. Magnetic studies confirmed the antiferromagnetic exchange interactions between magnetic centers.

High-nuclearity transition-metal clusters have grown in the past decade in relation to their potential applications associated with aesthetically pleasing structures and their rich physical and chemical properties.[1-8] These materials display magnetic hysteresis below a blocking temperature, which motivated both physicists and chemists to further explore their potential applications in date storage, quantum computing or spintronics.[3] The nature of the ligands is crucial in governing the nuclearity and arrangement of the resulting molecular aggregates.[1] Indeed, several organic ligands have been used to date, from simple and flexible carboxylates[2] to more bulky and robust polyalcohols,[3] azidos,[4] oxime,[5] phosphonates[6] and Schiff bases,[7] all leading to interesting structural motifs with different physical properties. Transition metal clusters of these polydentate ligands displayed a surprising variety of structure, consisting of wheel Co_{12},[2] phosphonate cage Ni_8,[6] "bowls" Ni_{20},[7] metallomacrocycle Zn_7,[8] cyclic Cu_{16},[9] etc.

To seek a new route to the synthesis of polynuclear clusters, we recently begun to employ the polydentate ligand 4-bromo-benzohydroxamic acid (Scheme 1), which possessing two O- and one N- donors and could be an ideal choice for the synthesis of high-nuclearity coordination clusters. Notably, the hydroxamate ligands have keto-enol tautomerism, so they are capable of forming complexes with beautiful structures. The reported transition mental clusters of hydroxamate ligands are only confined to the butterfly-like Co_4 and Ni_4,[10] a rich variety of coordination modes Ni_7,[11] face-centered cube with two wings Co_{16}[12] and metallahelicate Cu_{28}.[13] However, hydroxamate bridged Ni_{14} or Co_{14} clusters have never been reported. Based on other ligands, a family of Ni_{14} clusters was reported by end-on azido/oximate bridges[4] and a Co_{14} cluster was synthesised with a new bis-triazolate ligand.[14] Herein, we demonstrate two novel Co_{14} and Ni_{14} clusters. They are packed in a distorted face-centered cubic patterns, with six metals on the faces are bridged by the novel body-centred μ_6-O^{2-}. To the best of our knowledge, this is the first structurally characterized Co_{14}/Ni_{14} cluster in hydroxamate chemistry.

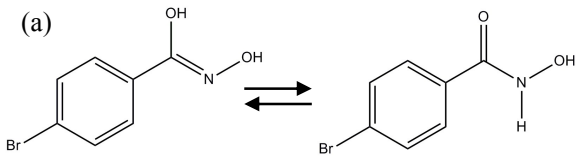

4-bromo-benzohydroximic acid (sH_2bha) 4-bromo-benzohydroxamic acid

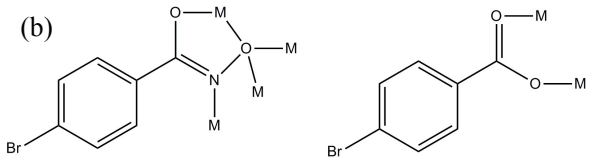

η^1: η^1: η^3: μ_4 (sH_2bha) η^1: η^1: μ_2 (sHba)

Scheme 1. (a)The keto-enol tautomerism of hydroxamate ligand and (b) Coordination modes found in 1-2 (M=Ni or Co)

The self-assembly reaction of sH_2bha, dppz (dipyrido[3,2-a:2′,3′-c]phenazine) , transition metal nitrate and Et_3N in 2:1:2:4 molar ratio in MeOH, EtOH, DMF and H_2O (10:5:5:2 v/v) yielded black (Co_{14})

Department of Chemistry, Collaborative Innovation Center of Chemical Science and Engineering, Nankai University, and Key Laboratory of Advanced Energy Materials Chemistry (MOE), Tianjin 300071, P. R. China. E-mail: guwen68@nankai.edu.cn, liuxin64@nankai.edu.cn

† X-ray crystallographic date for complex **1** and **2** in cif format (CCDC 1036508 and 1034226), Experimental procedures, Field-dependent magnetizations, Curie-Weiss plots of magnetic data, Cyclic voltammogram, Electronic absorption spectra, X-ray powder diffraction, IR spectroscopy and thermogravimetric analysis of complexes **1** and **2** available . See DOI: 10.1039/x0xx00000x

and green (Ni_{14}) block crystals, $[Co^{II}_{14}(\mu_6\text{-}O^{2-})(sbha)_{12}(sba)_2(DMF)_7(DMA)]\cdot(DMF)_8$ (1) and $[Ni^{II}_{14}(\mu_6\text{-}O^{2-})(sbha)_{12}(sba)_2(DMF)_8]$ (2) (sH_2bha = 4-bromo-benzohydroximic acid; sHba = 4-bromobenzene carboxylic acid; DMF = N,N-dimethylformamide; DMA = dimethylamine) (Scheme 2). Without adding dppz, no Ni_{14} or Co_{14} cluster was isolated in all tested conditions, the dppz may be the mineralizing agent because the presense of them slows the crystallization dynamics. X-ray diffraction experiments were employed to identify their structural properties.

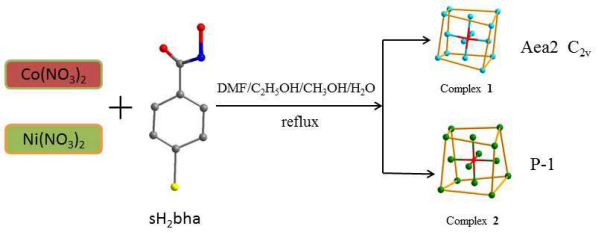

Scheme 2. Synthetic Routes for Complexes **1** and **2.**

Complex **1** crystallizes in the orthorhombic space group Aea2 with C_{2v}-symmetry operation. Its molecular structure (Fig.1b) consists of one μ_6-O^{2-}, twelve doubly deprotonated sbha ligands, two sba (Scheme 1), seven DMF, one DMA, as well as eight uncoordinated DMF molecules. The O^{2-} comes from deprotonated water. The sHba (4-bromobenzene carboxylic acid) was assumed to be originated from the hydrolysis of sH_2bha[12]. DMA (dimethylamine) was originated from the hydrolysis of DMF under alkaline condition.

There are eight crystallographically independent Co^{II} sites possessing distorted trigonal bipyramidal geometries (Co2, Co3, Co4) and distorted octahedral geometries (Co1, Co5, Co6, Co7, Co8) (Fig. 1b) for complex **1**. The five-coordinated Co2 and Co4 connect two oxygen atoms from one sbha bridge and two nitrogen atoms from two sbha bridges, and one oxygen atom from DMF, resulting in a distorted $[CoO_3N_2]$ trigonal bipyramidal coordination geometry. The coordination environment of Co3 is $[CoO_4N]$, provided by four oxygen atoms from two sbha bridges and one nitrogen atom from another sbha bridge. The $[CoO_5N]$ environment of Co1 has one more oxygen atom from sba bridge compared with the $[CoO_4N]$ environment of Co3. The six-coordinated Co5, Co6, Co7 and Co8 ions have similar distorted octahedral coordination environments. They connect with four oxygen atoms from four sbha bridges, one (μ6-O^{2-}), one oxygen atom from sba bridge or DMF or one nitrogen atom from dma (Fig. S3). The Co-N (sbha) and Co-O (sbha) separations span the range 2.010~2.174 Å and 1.918~2.248 Å. The average Co-O (μ_6-O^{2-}) bond distance is 2.148 Å. The Co-O (sba) bonds are 1.990 and 2.204 Å. The Co-O (DMF) bond distance span the range 2.055~2.078 Å. Co1~Co6 have their symmetric Co^{II} ions (Co1′~ Co6′), together with Co7 and Co8 which have no symmetry. The fourteen Co^{II} ions are packed in a distorted face-centered cubic (FCC) pattern, Co1~ Co4 and Co1′~ Co4′ ions occupy the FCC vertexes, while Co5, Co6, Co5′, Co6′, Co7 and Co8 ions are placed at the center of the FCC faces (Fig. 1c).

The cage-like $[Co_{14}N_{12}O_{13}]$ core of complex **1** contains twelve η^1:η^1:η^3:μ_4-sbha bridges, two η^1:η^1:μ_2-ba bridges and one (μ_6-O^{2-})

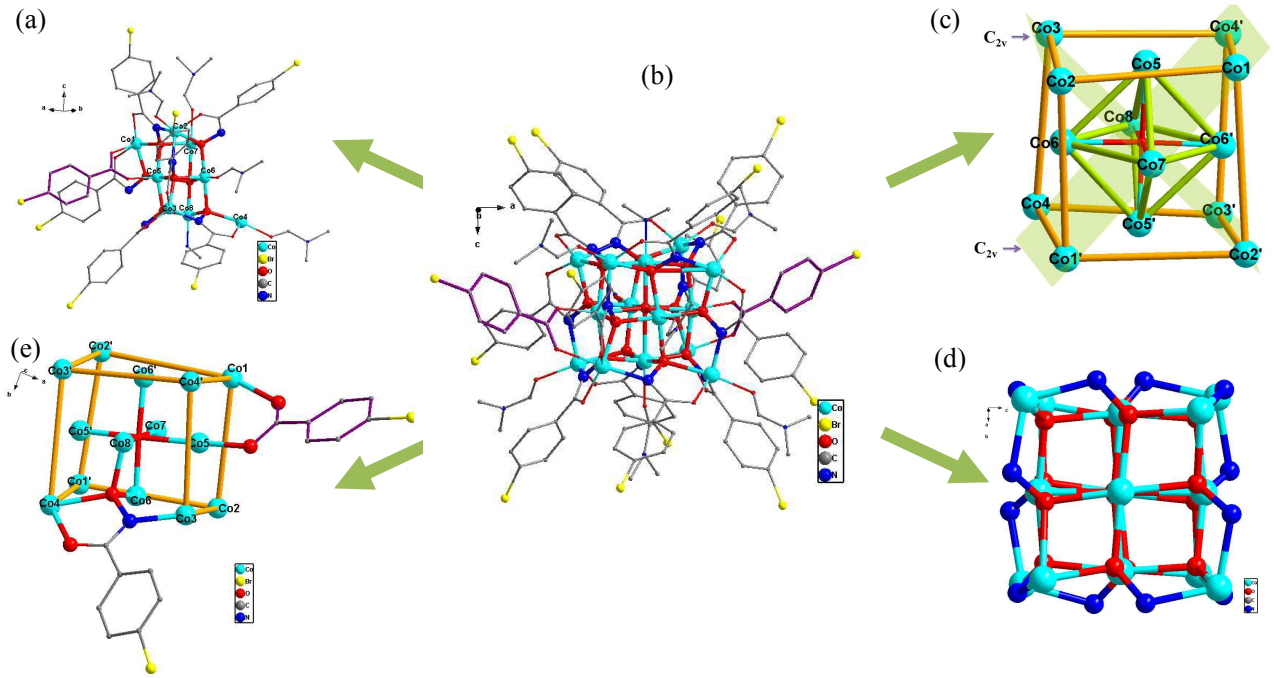

Fig. 1 (a) The asymmetric unit and (b) perspective views of complex **1**. (c) Perspective views of the core structure of complex **1.** (d) Metallic skeleton in **1** showing its face-centered cube topology with C_{2v} symmetry planes. (e) Views of structure of complex **1** with only one sbha one sba bridging ligands shown for clarity. Color key: Co, sky blue; O, red; N, blue; C, grey; Br, yellow. The color of the bonds of sba ligands is violet. H atoms are omitted for clarity.

Journal Name

COMMUNICATION

bridge (Fig. 1d, Fig. 1e and Fig. S2). The Co^{II} ions are bridged by the sbha ligands, the Co-O-N and Co-N-O bond angles span the range 108.6-125.9º and 108.5-111.4º. Co1 on the vertex and Co5 on the face are also bridged by the sba ligand, with the Co-O-C bond angles are 124.5º and 128.7º (Fig. 1e). The six Co^{II} ions on the faces were bridged by the body-centred (μ_6-O^{2-}), forming a regular octahedral geometry (Fig. 1c). For the Co^{II} ions on the adjacent faces, the Co-(μ_6-O^{2-})-Co bond angles show values 85.8º-94.1º. For the Co^{II} ions on the opposite faces, the Co7-(μ_6-O^{2-})-Co8 angle is 180.0 Å, while the Co5-(μ_6-O^{2-})-Co5′ and Co6-(μ_6-O^{2-})-Co6′ angles are 172.8 Å and 171.7 Å.

The interesting feature of complex **1** is that the regular octahedral geometry bridged by the body-centred (μ_6-O^{2-}) is trapped in a distorted cubic geometry hole as a "guest". The distorted cubic geometry Co-Co edge dimension and Co-Co-Co angles span the range 4.768-5.080 Å and 80.67-99.21º, and the dihedral angles of adjacent faces span the range 86.5-97.8º. The regular octahedral geometry Co-Co edge dimension and Co-Co-Co angles span the range 3.075-3.176 Å and 58.54-61.78º. The distances of the two Co on the opposite faces are 4.284-4.485 Å, slightly shorter than the cubic geometry Co-Co edge dimension (Fig. 1c).

Complexes **1** and **2** all contain fourteen transition metal ions, but the structures of them are different. Complex **2** crystallizes in the triclinic space group P-1 with no symmetry, which molecular structure (Fig. 2a) consists of one (μ_6-O^{2-}) bridge, twelve doubly deprotonated sbha ligands, two sba ligands, as well as eight DMF. Complex **2** has fourteen crystallographically independent Ni^{II} sites, of which six Ni^{II} ions are five-coordinated with distorted trigonal bipyramidal geometries and eight Ni^{II} ions are six-coordinated with distorted octahedral Geometries. The Coordination environments of

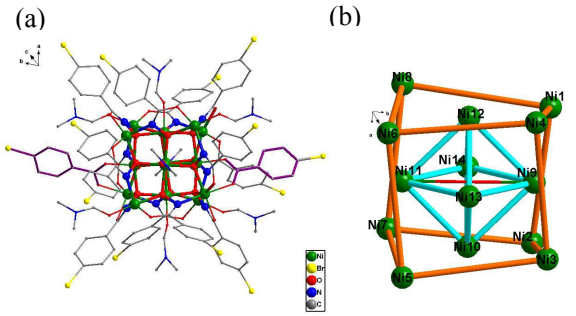

Fig. 2 (a) Perspective views of complex **2**. (b) Metallic skeleton in **2** showing its face-centered cube topology. Color key: Ni, green; O, red; N, blue; C, grey; Br, yellow. The color of the bonds of sba ligands is violet. H atoms are omitted for clarity.

the metal atoms are shown in the sopporting information(Fig. S5). The cage-like $[Ni_{14}N_{12}O_{13}]$ core of complex **2** contains twelve η^1:η^1:η^3:μ_4-sbha bridges, two η^1:η^1:μ_2-sba bridges and one body-centred (μ_6-O^{2-}) bridge. The fourteen Ni^{II} ions are packed in a distorted face-centered cubic (FCC) pattern. Ni1-Ni8 ions occupy the FCC vertexes, while Ni9-Ni14 ions are placed at the center of the FCC faces(Fig. S4).

The Ni^{II} ions are bridged by the sbha ligands, the Ni-O-N and Ni-N-O bond angles span the range 108.3-125.2º and 106.8-108.6º. The Ni^{II} ions (Ni1, Ni6) on the vertexes and ones (Ni9, Ni11) on the faces are also bridged by the sba ligands, with the average Ni-O-C bond angle is 126.5º (Fig. S4a). Six Ni^{II} ions on the faces are bridged by (μ_6-O^{2-}) with (μ_6-O^{2-})-Ni bond distance span the range 2.147-2.171 Å, forming a regular octahedral geometry (Fig. 2b). To the best of our knowledge, no clusters based on body-centred (μ_6-O^{2-}) bridged [Ni_6(μ_6-O^{2-})] has been reported to date. For the Ni^{II} ions on the adjacent faces, the Ni-(μ6-O^{2-})-Ni bond angles show values 89.3º-90.7º. For the Ni^{II} ions on the opposite faces, the Ni-(μ_6-O^{2-})-Ni angles are 179.2-179.4 Å. The distorted cubic geometry Ni-Ni edge dimension and Ni-Ni-Ni angles span the range 4.723-4.892 Å and 76.31-102.52º. The dihedral angles of the distorted cubic geometry span the range 89.3-91.1º. Complex **2** is much closer to regular FCC structure compared with complex **1**. The regular octahedral geometry Ni-Ni edge dimension and Ni-Ni-Ni angles span the range 3.044-3.065 Å and 59.53-60.40º (Fig. 2b).

Direct current (dc) magnetic susceptibility measurements were performed on fresh samples of complexes **1**-**2** in the temperature range 2-300K, in a magnetic field of 1000 Oe. Fig. 3 shows the plot χ_MT versus T. Alternating current (ac) magnetic susceptibility studies show no slow relaxation of magnetization in complex **1** (Supporting Information, Fig. S9).

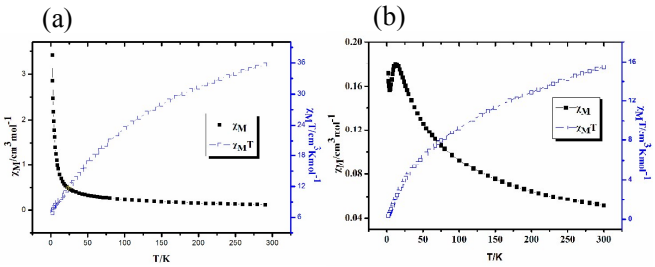

Fig. 3 (a) χ_MT versus T plots of complex **1**. (b) χ_MT versus T plots of complex **2**. Lines are guide to the eye.

The value of χ_MT at room temperature for complex **1** is 36.11 cm^3 K mol^{-1}, which is higher than the spin-only value of 14 high-spin, S=3/2, Co^{II} ions (26.25 cm^3 K mol^{-1}), indicating significant orbital contributions of Co^{II} ions. The value of χ_MT at room temperature for complex **2** are 15.40 cm^3 K mol^{-1}, which is consistent to the expected value for 14 isolated Ni^{II} ions (14.0 cm^3 K mol^{-1}). The χ_MT values for **1** and **2** decrease gradually upon lowering the temperature, reaching 6.81 cm^3 K mol^{-1} for **1** and 0.34 cm^3 K mol^{-1} for **2**. This behavior

shows that the magnetic exchange is dominated by antiferromagnetic interactions for complex **1** and **2**. The reciprocal molar susceptibilities in 30-300 K follow the Curie-Weiss Law of $1/\chi_M = (T-\theta)/C$ with Curie constants C=34.55 and 20.43 cm^3 K mol^{-1} and Weiss constants θ = -92.26 and -123.78 K for complexes **1** and **2**, respectively (Supporting Information, Fig. S7 and Fig. S8). The negative θ value of complex **1** suggests an antiferromagnetic interaction between the Co^{II} centers and/or the spin-orbit coupling effect of Co^{II}. The negative θ value of complex **2** suggests an antiferromagnetic interaction between the Ni^{II} centers. Because of the large size and complexity of the clusters, however, fitting of the experimental magnetic date could not be performed to determine the pairwise exchange interactions.

The electrochemical properties of **1** were examined by cyclic voltammetry CH_2Cl_2 containing 0.1 M n-Bu_4NPF_6 in the potential range from –2 to +2 V with a scan rate of 100 mV s^{-1} (Fig. S10). The complex exhibited one ill-defined irreversible reduction processes at approximately –1.25 to –0.5V versus saturated calomel electrode (SCE), which may correspond to the reduction processes of the ligand. A clear broad oxidation peak at 0.7 V vs. SCE was attributed to the irreversible oxidative process of Co^{II} to Co^{III}.[16] Complex **2** exhibited one ill-defined irreversible reduction processes at approximately –1.25 to –0.5V vs. SCE, whereas no visible oxidation wave was apparent (Supporting Information, Fig. S11).

In conclusion, two novel body-centred (μ_6-O^{2-}) bridged Co_{14} and Ni_{14} hydroxamate clusters were synthesized and they were packed in face-centered cubic (FCC) patterns. For the 4-bromo-benzohydroxamic acid ligand, they are the first reported clusters, which were characterized by magnetism, cyclic voltammetry, electronic absorption spectroscopy, thermogravimetric analysis, X-ray powder diffraction and IR spectroscopy. Structural investigation reveals some interesting geometrical features in the molecular cores and the magnetic exchange is dominated by antiferromagnetic interactions between magnetic centers. Cyclic voltammetry of complex **1** showed an irreversible oxidation at 0.7 V versus saturated calomel electrode.

Acknowledgements

This work was supported by the National Natural Science Foundation of China (no. 21371103).

Notes and references

1 R. Chakrabarty, P. S. Mukherjee and P. J. Stang, Chem. Rev., 2011, 111, 6810; S. Seidel, P. J. Stang, Acc. Chem. Res., 2002, 35, 972-983; T. R. Cook, R. Y. Yang and P. J. Stang, Chem. Rev., 2013, 113, 734-777.

2 P.R. Wei, T. W. Mak and D. A.Atwood, Inorg. Chem., 1998, 37, 2605-260; X. J. Lei, M. Y.Shang, A.Patil, E. E.Wolf and T.P.Fehlner, Inorg. Chem., 1996, 35, 3217-3222; E. Colacio, G. P. Costes, R. Kivekas, J. P.Laurent and J. Ruiz, Inorg. Chem., 1990, 29, 4240-4246.

3 A. J. Tasiopoulos, S. P. Perlepes, Dalton Trans., 2008, 5537-5555.

4 J. Esteban, L. Alcazar and M. Monfort, Inorg. Chem., 2012, 51, 5503-5505; D. I. Alexandropoulos, L. C. Silva, A. Escuer and T. C. Stamatatos, Chem. Eur. J., 2014, 20, 13860-13864.

5 R. Inglis, C. J. Milios, L. F. Jones, S. Piligkos and E. K. Brechin, Chem. Commun., 2012, 48, 181-190.

6 S. K. Langley, M. Helliwell, S. J. Teat and R. P. Winpenny, Inorg. Chem., 2014, 53, 1128-1134. J. A. Skeikh, A. Adhikary, H. S. Jena, S. Biswas and S. Konar, Inorg. Chem., 2014, 53, 1606-1613.

7 K. I. Alexopoulou, A. Terzis, C. P. Raptopoulou, V. Psycharis, A. Escuer and S. P. Perlepes , Inorg. Chem., 2015, 54, 5615–5617.

8 P. D. Frischmann, A. J. Gallant, J. H. Chong and M. J. MacLachlan, Inorg. Chem., 2008, 47, 101−112.

9 G. A. Craig, M. Schütze, D. Aguilà, O. Roubeau, J. Ribas-Ariño, S. Vela, S. J. Teat and G. Aromí, Inorg. Chem., 2014, 53, 3290−3297.

10 R. Tirfoin, L. M. Chamoreau, Y. L. Li, B. Fleury, L. Lisnard and Y. Journaux, Dalton Trans., 2014, 43, 16805-16817; J. Y. Xu, H. B. Song, G. F. Xu, X. Qiao, S. P. Yan and D. Z. Liao, Chem. Commun., 2012, 48, 1015-1017.

11 D. Gaynor, Z. A. Starikova, S. Ostrovsky, W. Haasec and K. B. Nolan, Chem. Commun., 2002, 506-507.

12 Y. Y. Cao, Y. M. Chen, L. Li, D. D. Gao, W. Liu, H. L. Hu, W. Li and Y. H. Li, Dalton Trans., 2013, 42, 10912-10918.

13 Y. H. Johnson, J. W. Kampf and J. W. Pecoraro, Angew. Chem. Int. Ed., 2003, 42, 546-549.

14 F. P. Huang, P. F. Yao, H. Y. Li, Q. Yu, H. D. Bian and H. Liang, Chem. Commun., 2015,51, 7598-7601.

15 M. Mannini, F. Pineider, P. Sainctavit, C. Danieli, E. Otero, C. Sciancalepore, A. M. Talarico, M. A. Arrio, A. Cornia, D. Gatteschi and R. Sessoli, Nat. Mater., 2009, 8, 194-197; M. N. Leuenberger, D. Loss, Nature, 2001, 410, 789-793.

16 Y. L. Bai, X. L. Bao, S. R. Zhu, J. H. Fang, M. Shao and H. Y.Shi, Eur. J. Inorg. Chem., 2014, 1275-1278; K. Dimitrou, J. S. Sun, K. Folting, G. Christou, Inorg. Chem.1995, 34, 4160–4166.

17 K. I. Alexopoulou, A. Terzis, C. P. Raptopoulou, V. Psychairs, A. Escuer and S. P. Perlepes, Inorg. Chem., 2015, 54 , 5615–5617.

18 M. L. Cao, J. J. Wu, H. J. Mo and H. J. Ye, J. Am. Chem. Soc., 2009, 131, 3458–3459.

19 A. Pathak, V. L. Blair, R. L. Ferrero, M. Mehring and P. C. Andrews, Chem. Commun., 2014, 50, 15232-15234.

20 F. H. Zhao, H. Li, Y. X. Che, J. M. Zheng, V. Vieru and L. F. Chibotaru, Inorg. Chem., 2014, 53, 9785-9799.

21 J. Esteban, M. F. Bardia, J. S. Costa, S. J. Teat and A. Escuer, Inorg. Chem., 2014, 53, 3194-3203.

22 J. Jankolovits, J. W. Kampf and V. L. Pecoraro, Inorg. Chem., 2014, 53, 7534-7546.

23 R. Hernandez-Molina, A. Mederos, Comprehensive Coordination Chemistry II, 2004, 1, 411 – 446.

Two novel body-centred (μ_6-O^{2-}) bridged Co_{14}/Ni_{14} hydroxamate clusters have been synthesized. They are packed in distorted face-centered cubic (FCC) patterns